JOURNAL OF MATERIALS SCIENCE **34** (1999) 3769–3778

Pressure induced amorphization in calcium phosphates

S. N. VAIDYA*, V. SUGANDHI‡
*Condensed Matter Physics Division, ‡Spectroscopy Division,
Bhabha Atomic Research Centre, Trombay, Mumbai-400 085, India
E-mail: snvaidya@apsara.barc.ernet.in

Polycrystalline hydroxylapatite (HA), hydrated tricalcium phosphate (HTCP), α tricalcium phosphate (α TCP), dicalcium phosphate dihydrate (DCPD) and dicalcium phosphate anhydrous (DCPA) were subjected to various pressures upto 10 GPa and the retrieved materials were examined by XRD and FTIR. These compounds showed amorphization at pressures upto 10 GPa, the pressure being lowest for HTCP and DCPA. At intermediate pressures, the amorphous phase obtained was anisotropic. Significant changes in the infrared spectra were observed in all materials except DCPA. These changes are due to the lowering of site symmetry on amorphization. © *1999 Kluwer Academic Publishers*

1. Introduction

There are several investigations on biocompatibility and clinical evaluations of hydroxylapatite (HA), tricalcium phosphate (TCP) and bone cements prepared from the mixtures of calcium phosphates [1]. Several composites [2] and ceramics [3, 4] derived from calcium phosphates and hydroxylapatite have been found to be biocompatible and are used in oral and prosthetic surgery and bone augmentation. The experimental studies on the formation of hydraulic calcium phosphate cements (CPC) have shown that in the early stages the material formed is in the amorphous state and over a period of four to thirty weeks it transforms to crystalline HA or octacalcium phosphate (OCP) [5, 6]. The properties of the CPC formed depend on a number of factors [7] such as the pH, temperature, presence or absence of certain ions such as Mg^{+2} and PO_4^{-3} and on the crystal structure of the reactants. The amorphous phase occurs in the early stages of formation, while the preparation of highly crystalline form often requires aging and extensive boiling of the precipitate or preparation under hydrothermal conditions [8].

We have reported earlier observation of crystalline to amorphous (c→a) transition in HA at a pressure of about 10 GPa [9]. Later we reported preliminary studies on pressure induced c→a transition in α tricalcium phosphate (α TCP), dicalcium phosphate dihydrate (DCPD) and anhydrous dicalcium phosphate (DCPA) [10]. It has been suggested that the pressure induced c→a transitions in $Ca(OH)_2$, $Mg(OH)_2$, $Ni(OH)_2$ and serpantine $3MgO{\cdot}2SiO_2{\cdot}2H_2O$ is probably caused by the expulsion of water at high pressures [11]. On the other hand, the c→a transition in $LiKSO_4$ and $AlPO_4$, which consists of an open network structure and are made up of two types of structural units having different compressibilities, is attributed to polyhedral tilt mechanism [12–15]. The crystal structures of calcium phosphates are also made up of loosely packed polyhedra. The polyhedra are arranged in columns in HA and TCP, in layered structures in DCPD and as inter-connected chains in DCPA. For the sake of completeness we have also investigated hydrated tricalcium phosphate (HTCP) which has a structure closely related to that of HA. The high pressure studies on calcium phosphates thus give an opportunity to study correlation between the pressure induced changes and the loosely packed crystal structures of these compounds.

The paper is arranged as follows. The experimental details pertaining to the preparation of materials, techniques used for characterisation and for high pressure investigations are given in Section 2. HTCP and HA have remarkable similarities. In Section 3 we discuss the experiments which bring out similarities and differences between HTCP and HA. In Section 4 we discuss the crystal structures and the results of high pressure studies on HTCP, HA, αTCP, DCPD and DCPA. Significant changes in the infrared spectra were observed for all materials except DCPA. In Section 5 we summarize the results and discuss the role of crystal structure in understanding the trends in the pressure induced c→a transitions.

2. Experimental techniques

HA used was prepared from $Ca(OH)_2$ and dilute H_3PO_4 in molar ratio 5 : 3 while maintaining pH > 7, following standard procedures, namely, slow addition of reactants, constant stirring, boiling and aging of the precipitate [9]. HTCP, DCPD and DCPA were analar grade materials from commercial sources. α TCP was prepared by heating HTCP to 1250 °C for 5 h.

The materials were characterised by X-ray powder diffraction (XRD) and Fourier transform infrared (FTIR) spectroscopic techniques. The X-ray diffraction patterns were recorded with CuK_α radiation using

a Philips PW 1820 wide-angle goniometer mounted on PW 1729 X-ray generator. The data were processed using a PW 1710 microprocessor coupled to a PC AT. The XRD patterns of all these materials matched well with those reported in the literature. FTIR studies were performed using a BOMEM DA3.003 spectrometer with mercury cadmium telluride (MCT) and deuterated triglycine sulphate (DTGS) detectors. For each sample 200 scans were accumulated with 1 cm^{-1} resolution using KBr pellets containing 1% sample. All spectra were recorded in vacuum in transmittance mode with pure KBr as reference. The FTIR studies showed carbonate bands at ~1400 cm^{-1} in HA, HTCP and DCPA but not in DCPD and α TCP. The infrared bands observed with our materials agreed well with the earlier reports on HA, α TCP and DCPD [16–18].

High pressure experiments employed Bridgman anvils having face diameter 12.7 mm and pyrophyllite gaskets having 12.7 mm o.d. × 5.3 mm i.d. × 0.5 mm height for experiments upto 8 GPa [19] and anvils having face diameter 6.3 mm and pyrophillites gaskets having 6.3 mm o.d. × 3 mm i.d. × 0.5 mm height for higher pressures upto 10.5 GPa [20]. The 0.45 mm thick compressed discs of the starting materials were placed in the centre of the pyrophillite gasket and kept at a desired pressure for 72 h. The Bi I-II and III-V transitions at 2.55 and 7.67 GPa were used for the pressure calibration of anvils.

3. Thermophysical studies on hydroxylapatite (HA) and hydrated tricalcium phosphate (HTCP)

Netzsch thermobalance Model STA 409 was used for simultaneous differential thermal analysis and thermogravimetric analysis (DTA-TG) experiments. Differential temperature sensor consisted of Pt/Pt-10%Rh thermocouples. Specimens of HA and HTCP dried at 100 °C were used. Fig. 1 shows the DTA-TG curves obtained at a heating rate of 10 K min. It is seen that both HA and HTCP show an endothermic peak upto about 200 °C followed by an exothermic behaviour from 200 to 500 °C. The endotherm is associated with the loss of adsorbed water. This type of behaviour has been reported in HA by Lin *et al.* [21] who attribute the exotherm to be agglomeration of ultrafine powders to reduce surface energy. In separate experiments specimens of HTCP and HA were heated at 150 and 200 °C in alumina boats for two hours and the XRD pattern of powders at room temperature were recorded. The materials retrieved from these temperatures was crystalline. We therefore attribute the exotherm to aggregation of microcrystallites as has been reported in HA [21]. HTCP and HA show similar dehydration characteristics and weight loss of approximately 4% upto 600 °C. It is seen that HA remains stable upto about 1100 °C and above this temperature it shows an exothermicity due to OH bond release. HTCP shows a plateau in

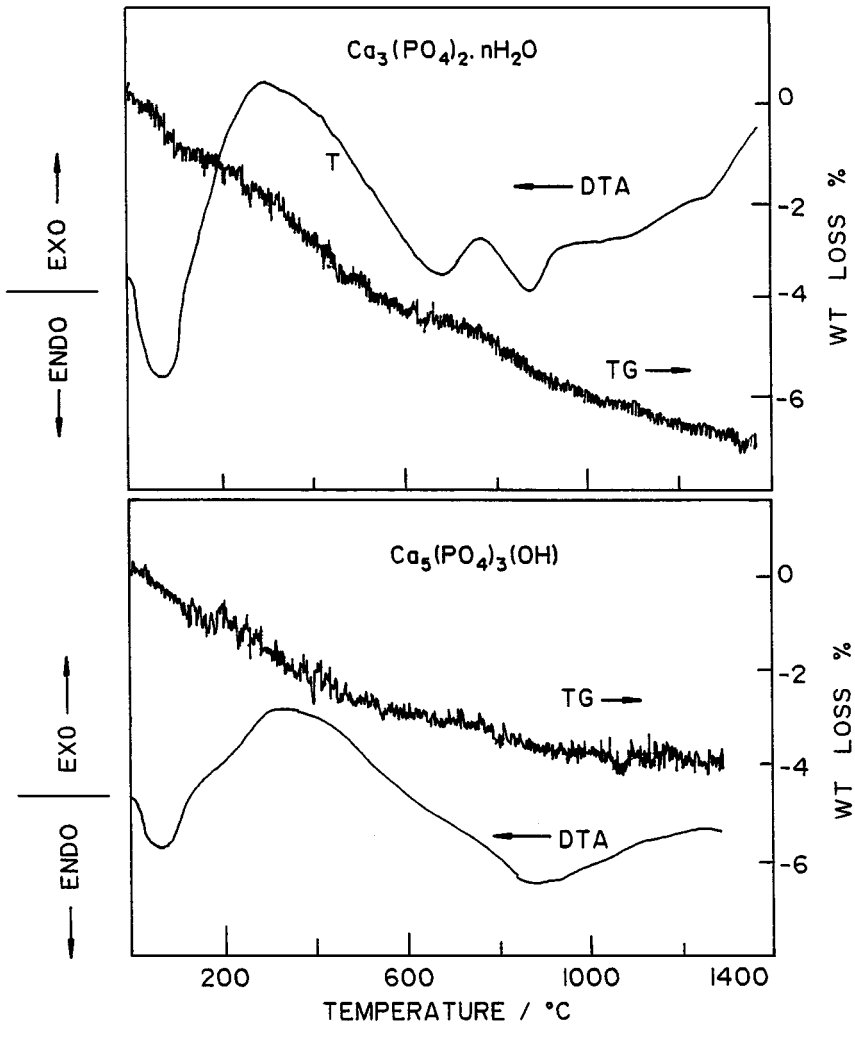

Figure 1 Differential thermal analysis and thermogravimetric analysis curves for (a) hydroxylapatite and (b) hydrated tricalcium phosphate.

the TG curve between 600 and 800 °C, as it gradually transforms to β TCP. The transformation is complete at 900 °C. There is an additional weight loss of 1.3% above 600 °C as it transforms to anhydrous tricalcium phosphate. On the basis of a total weight loss of about 6% the molecular formula of HTCP used in our experiments can be written as $Ca_3(PO_4)_2$ $1.1H_2O$. The transition to β TCP around 900 °C and to α TCP around 1280 °C is marked by the exothermic change in the DTA curve.

HTCP was heated in an alumina crucible at different selected temperatures for twenty four hours and furnace cooled. The XRD patterns of the retrieved materials were taken to identify the phases formed on heating HTCP at various temperatures. The results are summarized in Fig. 2. It is seen that HTCP heated to 635 °C for twenty four hours transforms into a mixture of HTCP, β TCP and an amorphous phase. The hump in the X-ray background indicates the pressure of amorphous phase. The HTCP $\rightarrow \beta$ TCP dehydration reaction is accompanied by fragmentation of material. The material heated to 920 °C for forty hours shows complete conversion to the β TCP phase and the narrow line width indicates high crystallinity of this material. At 1250 °C it shows transition to α TCP phase. A detailed description of TG/DTA of HTCP and HA was given to distinguish these two compounds which gave nearly identical XRD patterns.

HTCP was heated to 540 °C and furnace cooled. It gave an XRD pattern similar to that of starting HTCP. At this temperature, there is loss of adsorbed water and the composition as deduced from TG analysis is TCP $0.3H_2O$. The XRD pattern however is same as that of starting HTCP. In separate experiments

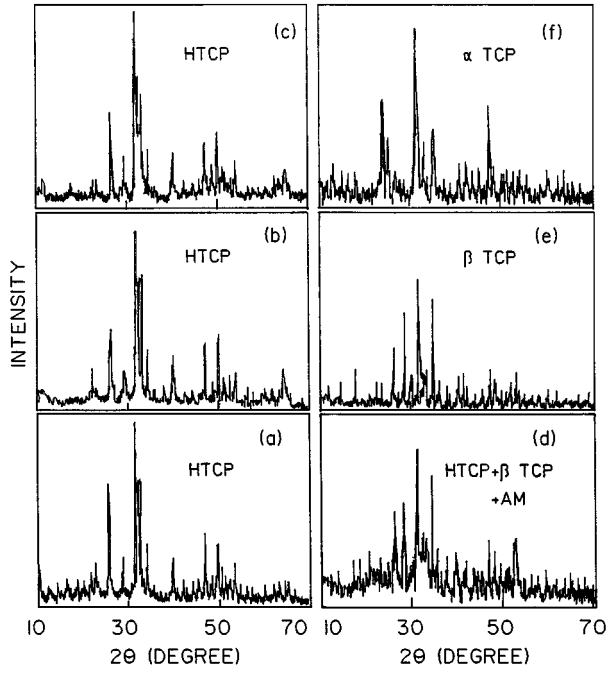

Figure 2 XRD patterns of hydrated tricalcium phosphate: (a) as prepared powder, (b) powder fired for 12 h at 120 °C, (c) at 540 °C, 12 h, (d) at 635 °C, 12 h, (e) at 900 °C, 12 h and (f) at 1250 °C, 24 h. The phases observed in the XRD pattern are identified. HTCP: hydrated tricalcium phosphate, TCP: tricalcium phosphate, Am: amorphous.

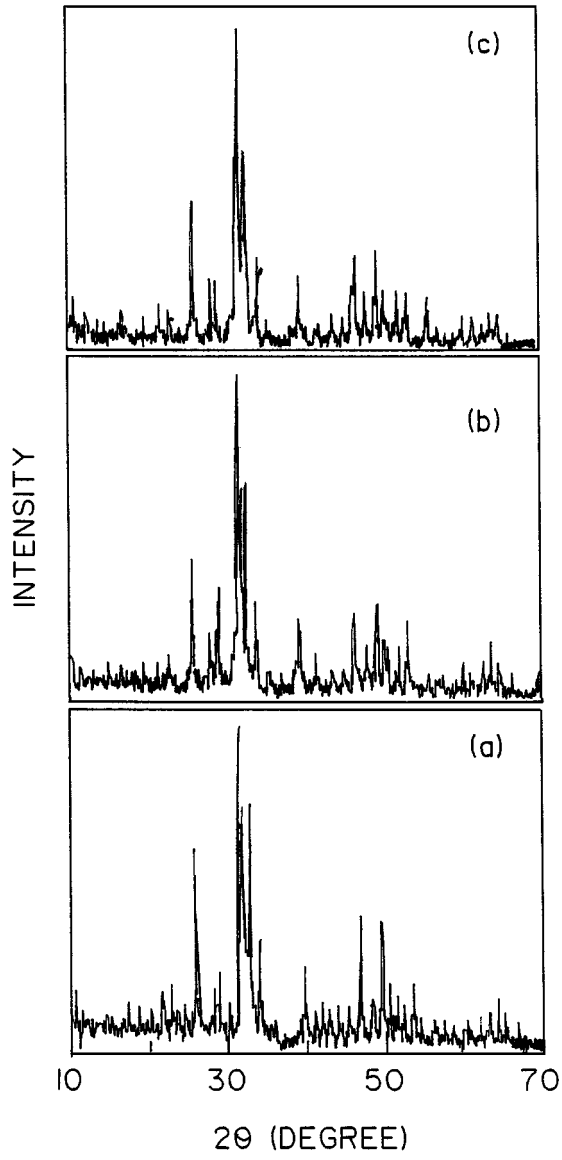

Figure 3 XRD pattern of hydrated tricalcium phosphate: (a) HTCP fired at 120 °C, (b) HTCP +1/3 mol % of $Ca(OH)_2$ fired at 460 °C, 24 h and (c) HTCP +1/3 mol % of CaF_2 fired at 460 °C, 24 h.

HTCP $\{Ca_3(PO_4)_2$ $1.1H_2O\}$ was mixed with $Ca(OH)_2$ and CaF_2 to produce composition with Ca/P ratio 5 : 3. The mixtures were heated to 460 °C for 24 h and furnace cooled. The XRD patterns obtained were similar to those of starting HTCP and diffraction lines corresponding to unreacted $Ca(OH)_2$ or CaF_2 were not observed (Fig. 3). These experiments bring out intrinsic stability of the HA type structure over the composition range $Ca_3(PO_4)_2$ $1.1H_2O$ to $Ca_3(PO_4)_2$ $0.3H_2O$ to $Ca_5(PO_4)_3(OH)$. The structure seems to tolerate Ca/P ratio 1.5 to 1.67 provided a certain minimum amount of water of hydration or hydroxyl groups are present. Posner *et al.* [22] first pointed out that HTCP also has structure similar to that of HA. Both HA and HTCP crystallize in the space group $P6_3/m$ and have similar lattice parameters. The cell parameters are given in the Table I. Two forms having formula TCP $0.5H_2O\{3Ca_3(PO_4)_2$ $0.5H_2O\}$ and TCP $2H_2O\{3Ca_3(PO_4)_2$ $2H_2O\}$ have been reported [23]. The crystal structure of HA has been solved and refined

TABLE I Latice parameters of calcium phosphates

	S.G.	Cell parameters nm	Crystal structure and references	JCPDF card. no
$Ca_5(PO_4)_3(OH)$ HA	$P6_3/m$	$a = .943$, $c = .688$	Columnar along *c*-axis [23]	9–432
$Ca_3(PO_4)_2nH_2O$ HTCP	$P6_3/m$	$a = .946$, $c = .688$	Similar to HA [23]	18–303
α $Ca_3(PO_4)_2$ α TCP	$P2_1/a$	$a = 1.288$, $b = 2.728$, $c = 1.522$, $\beta = 126°12'$	Similar to HA [26]	29–359
$CaHPO_4 2H_2O$ DCPD	I2/a	$a = 0.5812$, $b = 1.818$, $c = 0.6239$, $\beta = 111°25'$	Sheets of $CaPO_4$ [27]	11–293
$CaHPO_4$ DCPA	P1	$a = .69$, $b = .665$, $c = .70$ $\alpha = 96°21'$, $\beta = 103°54'$, $\gamma = 88°44'$	Interconnected chains of -Ca-PO_4- [28]	9–80

by X-ray diffraction and neutron diffraction techniques [24, 25]. However single crystal structure data is not available for HTCP.

The infrared spectra of HTCP and HA at atmospheric pressure are shown in Figs 6 and 7. The close similarity of the infrared spectra also suggests that both HA and HTCP have similar crystal structures.

4. Results and discussion

4.1. Hydroxylapatite (HA) and hydrated tricalcium phosphate (HTCP) $Ca_3(PO_4)_2 \cdot 1.1H_2O$

The structure of HA (S.G. $P6_3/m$) with $a = 0.943$, $c = 0.688$ nm consists of columns of skewed 3 Ca_{II}-O trigonal prisms around the 6_3 axis. A distinct feature of the structure is that the PO_4 tetrahedra do not share the oxygen atoms among them and are held together by the Ca_I atoms Fig. 4. The O_H oxygen atoms belonging to the OH group are situated with equal probability either little above or below the plane of Ca_{II} atoms on the 6_3 axis. Only in stoichiometric HA all the O_3 oxygen atoms are either above or below the plane of Ca_{II} atoms and the symmetry of the crystal is reduced in the new space group. HA has an anisotropic structure having columns of Ca atoms and PO_4 units along the *c* axis.

The X-ray powder data indicates that HTCP has structure similar to that of HA and the removal of OH as in α $Ca_3(PO_4)_2$ (Section 4.2) leads to monoclinic distortion of the cell. It seems that the water of hydration in HTCP $\{Ca_3(PO_4)_2 \cdot nH_2O\}$ restores the hexagonal symmetry. In the crystal structure of HTCP, the water molecules are probably on an average distributed over the sites which are occupied by the O_H atoms in HA and there are Ca atom vacancies at the Ca_I sites. The structure of HTCP bridges the structure between HA and α TCP. Vaidya *et al.* [9] have reported occurrence of a progressive irreversible c→a transition in HA with increasing pressure. The complete amorphization occurs above 10 GPa. It is seen (Fig. 5) that in HTCP amorphization sets in at a lower pressure of about 2 GPa.

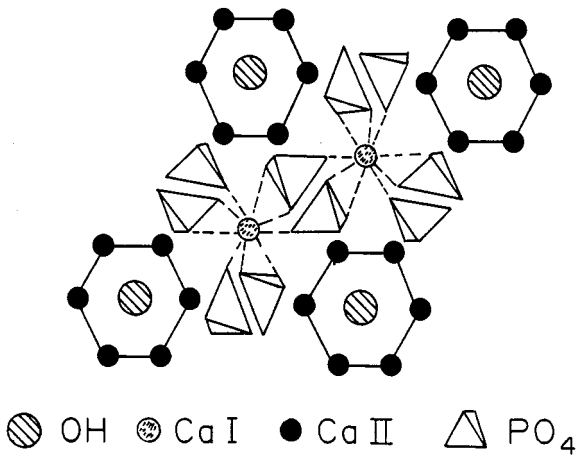

Figure 4 A projection of the crystal structure of hydroxylapatite on the (001) plane.

The infrared absorption frequencies and their assignments for various calcium phosphates investigated in crystalline state at 1 bar and in the pressure induced amorphous phase are given in Table. II. The infrared spectra of HA shown in Fig. 6 exhibits all the bands which have been reported by Baddiel and Berry [16] and Bertoluzza *et al.* [17]. The PO_4 ion in HA shows nine internal modes: symmetric stretch (ν_1), a doubly degenerate symmetric bend (ν_2), a triply degenerate asymmetric stretch (ν_3) and a triply degenerate asymmetric bend (ν_4). We have observed all the modes except the low lying ν_2 mode at <350 cm^{-1}. ν_3 (F_2) triply degenerate PO_4 stretch mode of phosphate occurs as a broad band from 1120 to 980 cm^{-1} in the crystalline phase becomes narrow in the amorphous phase. The PO_4 symmetric stretch (ν_1) at 959 cm^{-1}, the O-P-O bending mode ν_4 (F_2) from 605 to 550 cm^{-1} becomes weak but their position remain unchanged at c→a transition. The overtone or combination band originating from the components of ν_2 and ν_4 appearing at 1193 cm^{-1} becomes very weak in amorphous phase. The OH libration mode at 631 cm^{-1}, which is a weak band, remains unchanged.

The oxygen of the O-H groups O_H is located above or below triangles of Ca_{II} atoms. The geometry is similar to that found in $Ca(OH)_2$. Ca_{II}-O_H distance of 0.238 nm in HA is comparable to Ca-O distance 0.237 nm in $Ca(OH)_2$. O_H-O bond distance is 0.0999 nm in HA compared to 0.0984 nm in $Ca(OH)_2$, 0.0971 nm in OH^- radical and 0.958 nm in water. Baddiel and Berry [16] point out that rather small O_H-O distance between O_H and nearer of phosphate oxygens of 0.3068 nm in HA suggests the possibility of weak bonding.

In crystalline HA, due to hydrogen bonding the internal antisymmetric stretching of the OH ion ν_{OH} is observed at 3561 cm^{-1}. In $Ca(OH)_2$, $Mg(OH)_2$ and LiOH

TABLE II Observed vibrational frequencies and assignments of various calcium phosphates

	HA R_P	HA 10 GPa	HTCP R_P	HTCP 2 GPa	α TCP R_P	α TCP 10 GPa	DCPD R_P	DCPD 10 GPa	DCPA R_P	DCPA 10 GPa
ν_1 PO_4	959	959	961		959					
ν_3 F_2 PO_4	1120–980	1080-1000	1110–1020	1080–1000	1100–1000	1100–1020	1134, 1123 1057	1134, 1123 1057	1131, 1070	1131, 1070
ν_4 F_2 PO_4	605–550	605–550	602, 571	602, 571	603, 551	603, 551	576, 527	576, 527	573, 563 536	573, 563 536
OPO, bend	417, 370							417, 370	404	404
ν_{OH}	631	631	633	633						
Combination	1193		1200							
ν_{OH} stretch	3561	3561, 3673	3567	3565, 3678			3538, 3485	3538, 3485		
ν_{OH} stretch							3268, 3162	3268, 3162		
ν_{OH} bend							1650	1650		
PO-H stretch							2920	2920		
P-O symmetric stretch							1002, 990	1002, 990	996	996
P-OH stretch	870		874				876	876	892	892
POH in plane							1208			

HA: Hydroxylapatite, HTCP: Hydrated tricalcium phosphate, α TCP: α tricalcium phosphate, DCPD: Dicalcium phosphate dihydrate, DCPA: Dicalcium phosphate anhydrous.

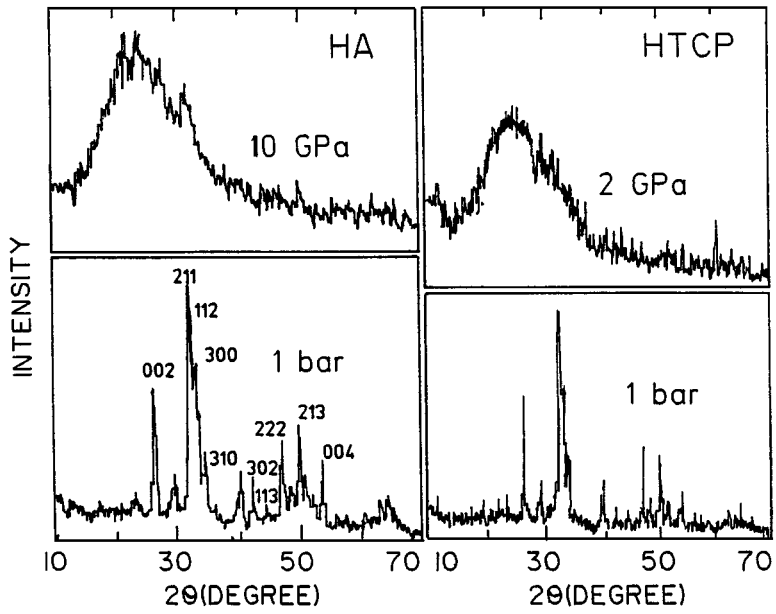

Figure 5 Effect of pressure on the XRD pattern of hydroxylapatite and of hydrated tricalcium phosphate at 1 bar and at high pressures.

which do not show hydrogen bonding, the stretching mode is observed at 100–140 cm^{-1} higher values instead. In amorphous HA, sharp peaks observed at 3561 and 3673 cm^{-1} indicate the existence of hydrogen bonded as well as non-bonded water in this phase.

The infrared spectra of HTCP is very similar to that of HA (Fig. 7). A wide ν_3 (F2) band occurs from 1110 to 1020 cm^{-1}, ν_1 at 961 cm^{-1} and ν_4 (F_2) band at 602, 571 cm^{-1} and combination band is seen at 1200 cm^{-1}. As in case of HA the ν_3 modes show pronounced narrowing at c→a transition. The OH libration mode occurs at 633 cm^{-1} and it remains unchanged. As in HA we observe antisymmetric stretching mode of OH at 3567 cm^{-1} in crystalline phase. In the amorphous phase two bands corresponding to bonded and non bonded water are observed at 3565 and 3678 cm^{-1}, respectively. In summary there is little that distinguishes the XRD and infrared features of HA and HTCP both in crystalline and amorphous phases. Only the pressure of c→a transition drops to a small value ∼2 GPa in the case of HTCP.

Sakuntala and Arora [26] have shown that at high pressures potash alum crystals having high initial orientational disorder show c→a transformation while crystals with low initial disorder do not. HTCP has a highly disordered HA type structure. The structure has some Ca_I atom vacancies and $1.1H_2O$ molecules which are probably distributed at random. The low amorphization pressure can be due to a high degree disorder in HTCP.

4.2. α tricalcium phosphate (α TCP)

α TCP crystallises in monoclinic system (S.G. $P2_1/a$) with $a = 1.288$, $b = 2.728$ and $c = 1.5219$ nms and $\beta = 126.2°$. Mathew *et al.* [27] have shown that this structure is closely related to the structure of HA when viewed along the *c* axis. In Fig. 8 is shown the outline of the subcell to bring out the similarity with the hexagonal structure of HA. The Ca and PO_4 ions are packed into two kinds of columns along the [001] direction with one column containing only the Ca atoms and the other containing both the Ca atoms and PO_4 tetrahedra

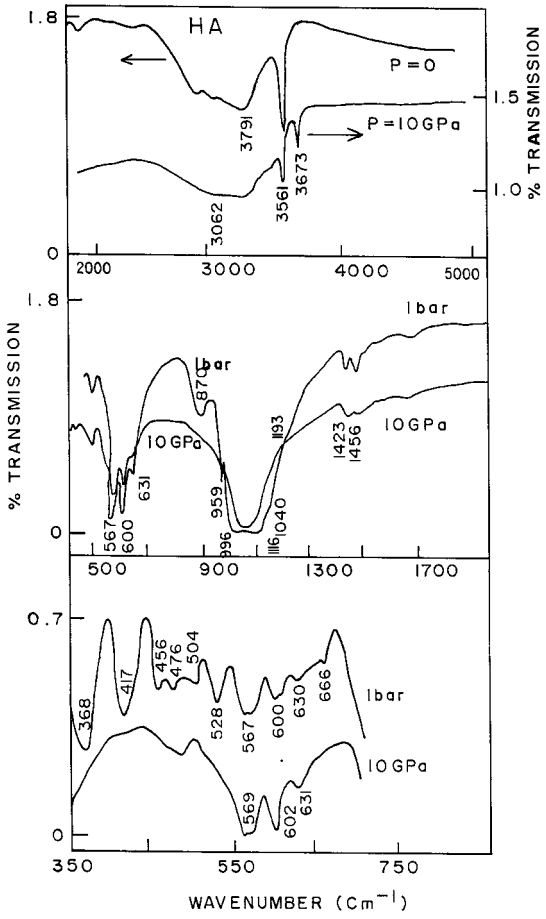

Figure 6 Effect of pressure on the FTIR spectrum of hydroxylapatite disc.

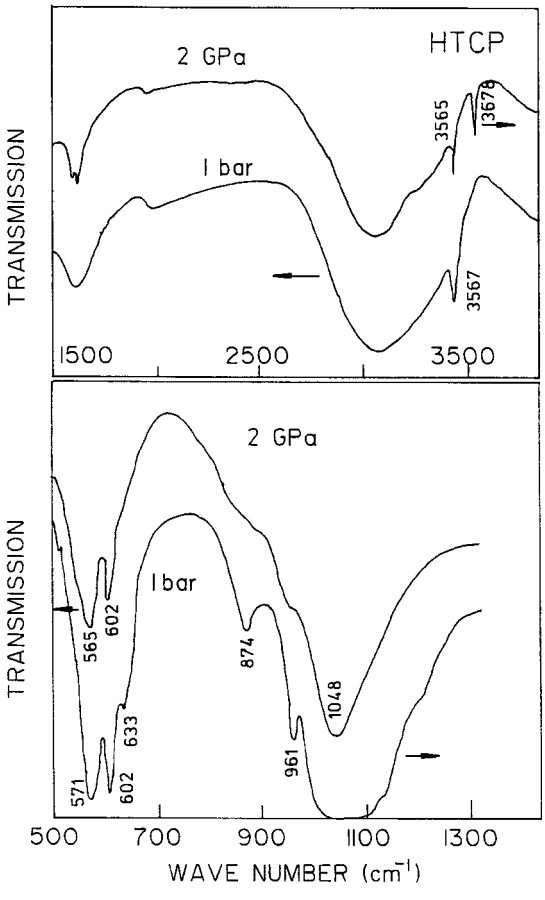

Figure 7 Effect of pressure on the FTIR spectrum of hydrated tricalcium phosphate.

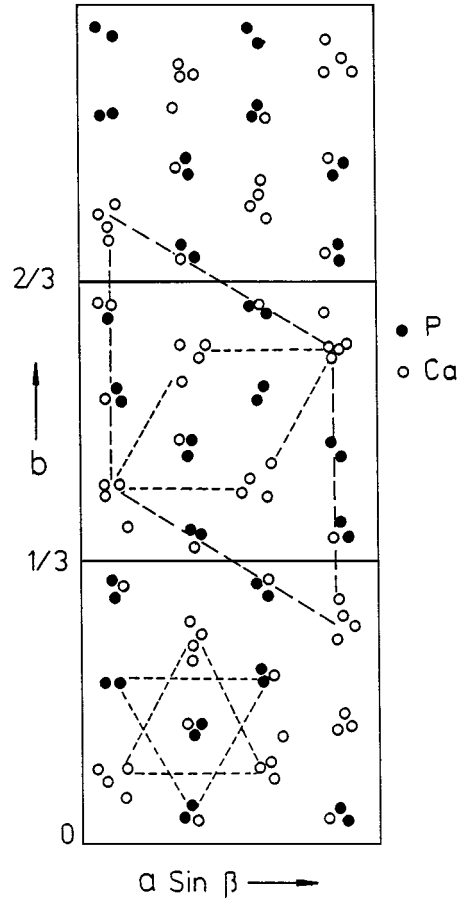

Figure 8 A projection of α $Ca_3(PO_4)_2$ structure on the (001) plane. Oxygen atoms of phosphate groups have been omitted. Dashed lines outline the cell corresponding to the structure of hydroxylapatite.

just as in HA. However in α TCP some of the Ca_I sites in the cation-anion columns are vacant.

The XRD pattern of the discs of α TCP subjected to various pressures are shown in Fig. 9. It is seen that long range disorder (LRD) which is characterised by increase in the X-ray background intensity at diffraction angles $2\theta < 30^\circ$ sets in at 2 GPa and it persists until 8 GPa. A maximum in the X-ray intensity at about 22° characteristic of amorphous phase is seen in α TCP pressurised to 10.5 GPa. Thus the transformation seems to be complete at about 10 GPa.

The infrared spectra of α TCP in crystalline and amorphous phases are shown in Fig. 10. α TCP shows a simple infrared spectra because there are no water or OH groups. Its spectra closely resembles that of HA without the modes due to OH vibrations. It shows a broad PO_4 stretch mode ν_3 (F_2) from 1100 to 1000 cm^{-1}. As in HA this mode becomes quite narrow in the amorphous phase. The PO_4 symmetric stretch ν_1 is seen as a shoulder at 959 cm^{-1} at STP. This mode merges with the PO_4 band in the amorphous phase. The OPO bend ν_4 (F_2) at 603 and 551 cm^{-1} becomes weak in the amorphous phase.

4.3. Dicalcium phosphate dihydrate (DCPD)

DCPD crystallises in monoclinic system (S.G.I2/a) with $a = 0.5812$, $b = 1.818$ and $c = 0.6239$ nms and $\beta = 111°25'$ [28]. As shown in Fig. 11, the structure is made up of corrugated sheets containing parallel chains

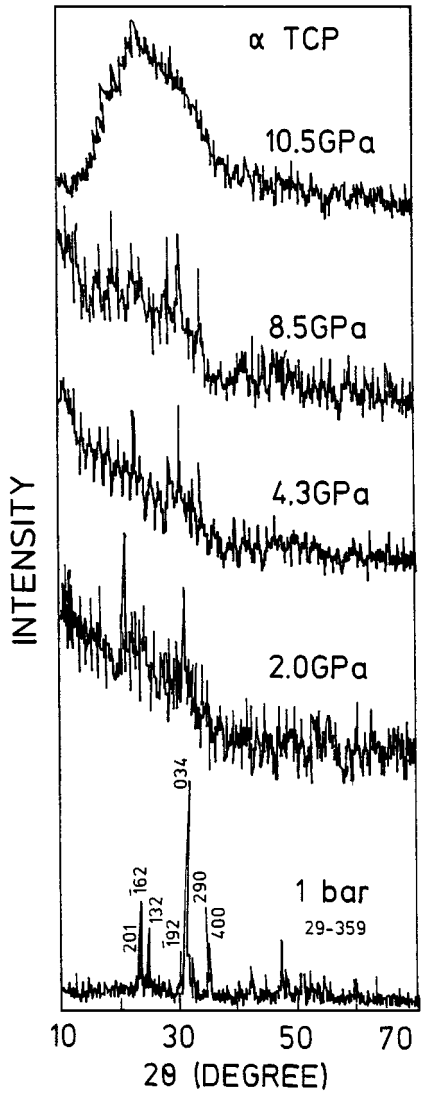

Figure 9 XRD patterns of α $Ca_3(PO_4)_2$ as a function of applied pressure.

of composition -PO_4-Ca-PO_4-Ca-. These corrugated sheet repeat themselves at a distance $b/2 = 0.579$ nm and are held together by water molecules which link a Ca atom and an oxygen atom in one sheet to an oxygen atom in the adjacent sheet. This structure has a close resemblance to the structure of gypsum $CaSO_4 \cdot 2H_2O$.

The XRD pattern of the discs of DCPD subjected to various pressures are shown in Fig. 12. All principal diffraction lines are seen at 2 GPa and a small increase in the background intensity for $2\theta < 40^\circ$ signals the onset of long range disorder. The number and intensity of the diffraction lines progressively decreases at 4.3 and 8.3 GPa, respectively, but the (020) line remains strong in all the pressurised specimens. DCPD pressurised to 10.5 GPa shows distinct pattern characteristic of an amorphous material. The (020) line which represents periodicity along the *b* axis is prominent even in the highly amorphized material obtained at 10.5 GPa. The evidence based on the XRD pattern suggests that the crystal structure of DCPD collapses in the plane of the corrugated sheets (*ac* plane) while it retains its periodicity along the *b* axis in the original structure.

The infrared spectra of DCPD (Fig. 13) showed all the bands reported by Casiani and Condrate [18]. The bands were assigned following Casiani and Condrate. DCPD contains two crystallographically distinct types

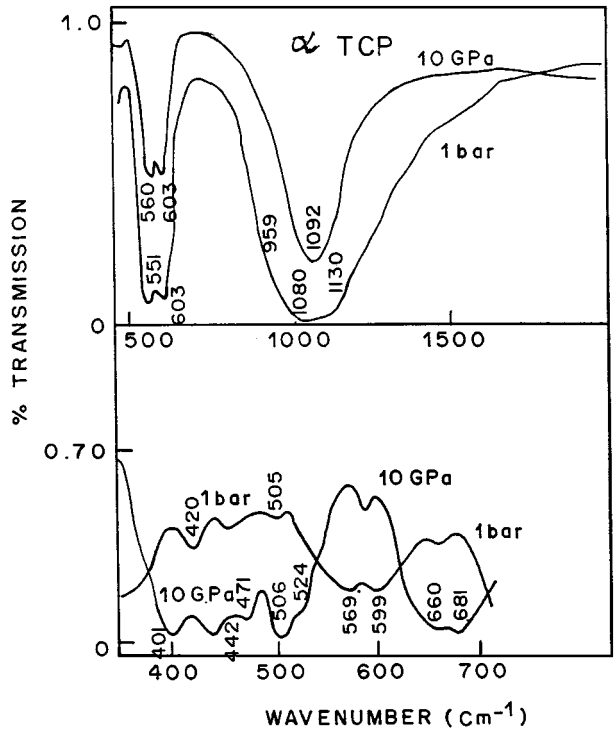

Figure 10 Effect of pressure on the FTIR spectrum of α $Ca_3(PO_4)_2$.

of water molecules having different absorption frequencies. They are doublets and are observed at 3538, 3485 and 3268, 3162 cm^{-1} respectively. These correspond to the stretching modes of water. The bending mode of water ν_2 is observed at 1650 cm^{-1}. The band position and intensity of these water bands do not change on amorphization. This supports the contention that the bonding provided by the water molecules between Ca and PO_4 sheets remains intact in the amorphous phase. The PO-H stretching mode at (ν_1) 2920 cm^{-1} (broad), the P-O symmetric stretching (ν_2) at 1002 (sh), 990 (s) and the P-OH stretching frequency (ν_3) at 876 cm^{-1} do not change significantly at c→a transition. The ν_3 (F_2) triply degenerate P-O stretch which gives a broad band in HA and α TCP shows splitting. This is because that each site group for the phosphate ion will split into fundamentals possessing A′ and A″-symmetry when one applies factor group analysis. As a consequence, we observe P-O stretch (ν_6) at 1134 (s), 1123 (sh) and 1057 cm^{-1} (s). The position and intensity of these bands is not much affected on amorphization. The in-plane-bending mode POH (ν_5) at 1208 cm^{-1} (weak sh) and the OPO(H) triply degenerate bending mode (ν_4 and ν_7) appearing at 576 cm^{-1} also do not change. The OPO symmetric bend (ν_8) vibrations appearing at 417 and 370 cm^{-1} which are not seen in the crystalline phase become intense in the amorphous phase. We find that below 500 cm^{-1} the infrared spectra of HA at one bar resembles that of DCPD at 10 GPa, while the infrared spectra of HA at 10 GPa resembles that of DCPD at 1 GPa. This result seemed unusual and so we repeated the experiments to confirm it.

4.4. Dicalcium phosphate anhydrous (DCPA)

The DCPA crystallises in triclinic system (S.G. P1) with $a = 0.690$, $b = 0.665$, $c = 0.700$ nm, $\alpha = 96^\circ 21'$,

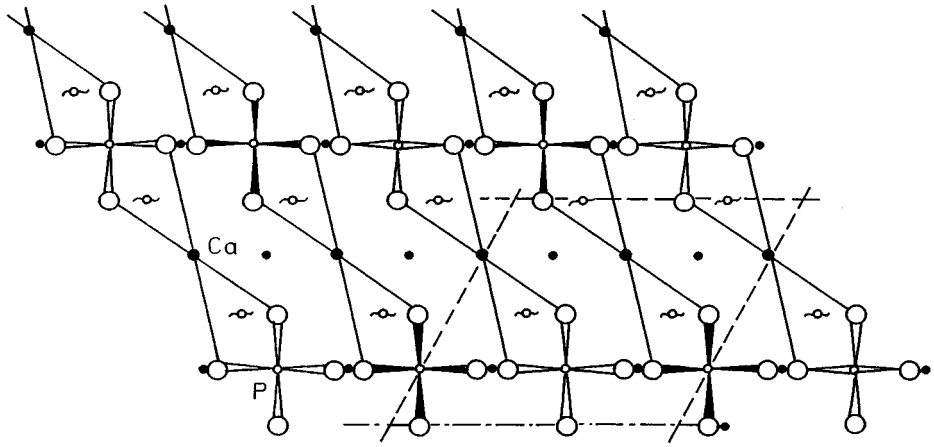

Figure 11 Projection of the structure of $CaHPO_4 \cdot 2H_2O$ on to a plane perpendicular to [101].

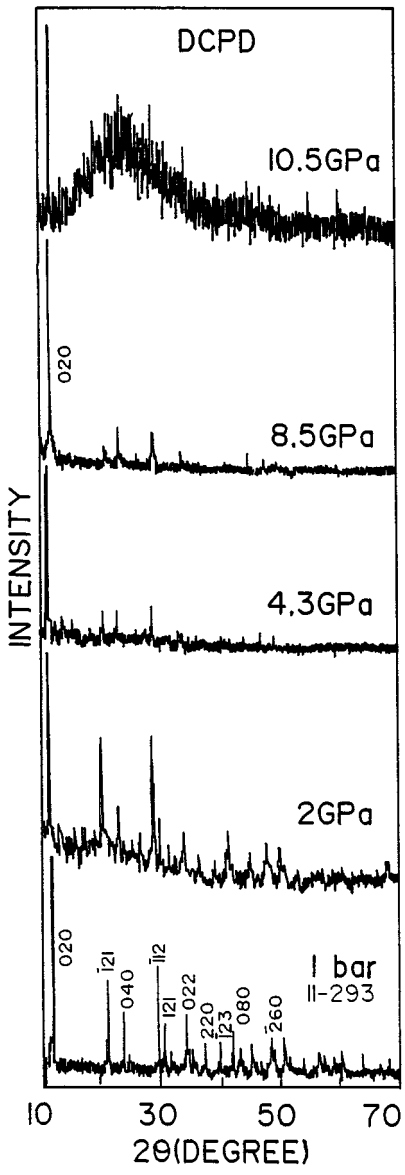

Figure 12 XRD patterns of $CaHPO_4 \cdot 2H_2O$ as a function of applied pressure.

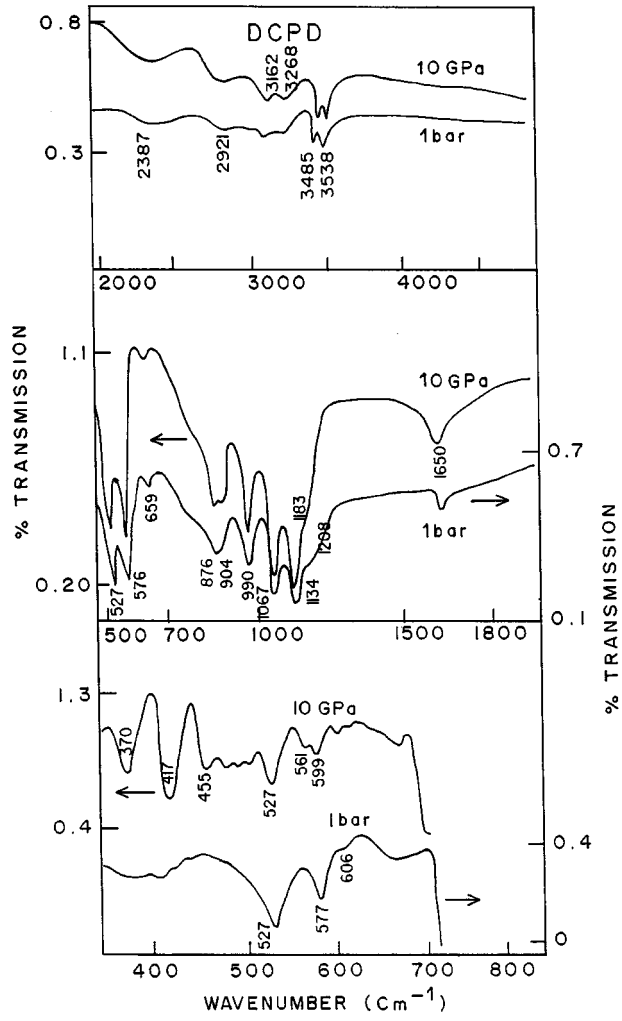

Figure 13 Effect of pressure on the FTIR spectrum of $CaHPO_4 \cdot 2H_2O$.

$\beta = 103°54'$ and $\gamma = 88°44'$ [29]. The structure consists of double chains of -Ca-PO_4-Ca- which extend along the *a* axis (Fig. 14). These chains are bonded transversely in the *b* direction forming a distorted sheet of atoms roughly in (001) plane. The calcium coordination polyhedra are unsymmetrical and co-ordination ranges from 6 to 9. The hydrogen atom probably lies between the oxygens of the neighboring PO_4 groups. This loosely packed structure consisting of a network of PO_4 tetrahedra which is held together by the Ca^{++} ions.

The XRD patterns of the discs of DCPA pressed to various pressures are shown in Fig. 15. It is seen that at 2 GPa, the intensity of the several XRD lines become weak and the background increases for $2\theta < 40°$. The (020) line remains strong as the structure collapses normal to the *b* axis and becomes partially amorphous at

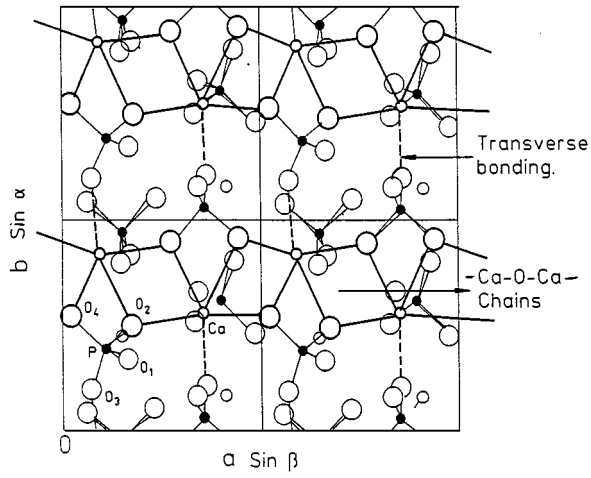

Figure 14 A projection of the structure of $CaHPO_4$ down the *c* axis.

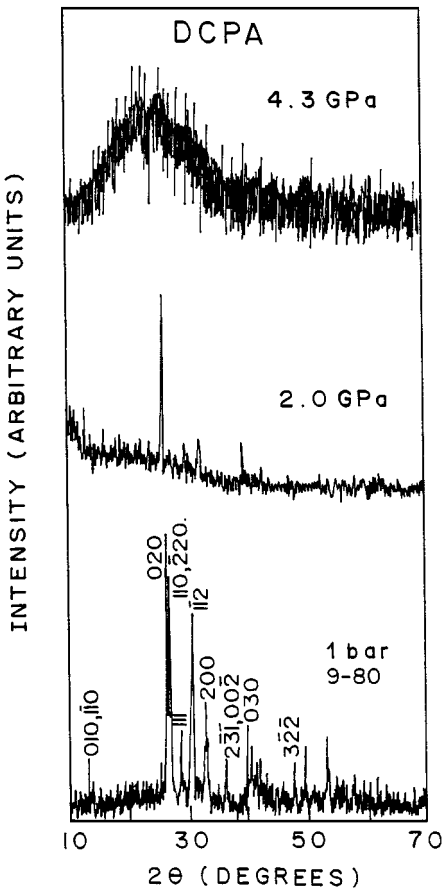

Figure 15 XRD patterns of $CaHPO_4$ as a function of applied pressure.

this pressure. The structure becomes fully amorphous at about 4 GPa.

The FTIR spectra of DCPA (Fig. 16) resembles that of DCPD which also has a low symmetry. The triply degenerate P-O stretching mode with F_2 symmetry (ν_3) are observed at 1131 and 1070 cm^{-1}. The P-O symmetric stretch mode (ν_1) is observed at 996 cm^{-1} and the P-OH stretch at 892 cm^{-1}. The asymmetric bend modes (ν_4) are seen at 573, 563 and 536 cm^{-1} and the OPO symmetric bend mode at 404 cm^{-1}. In this material the position and intensity of all the vibrations do not change significantly on amorphization. This is due to the low symmetry of the crystal structure and low site group symmetry of PO_4 groups in DCPA.

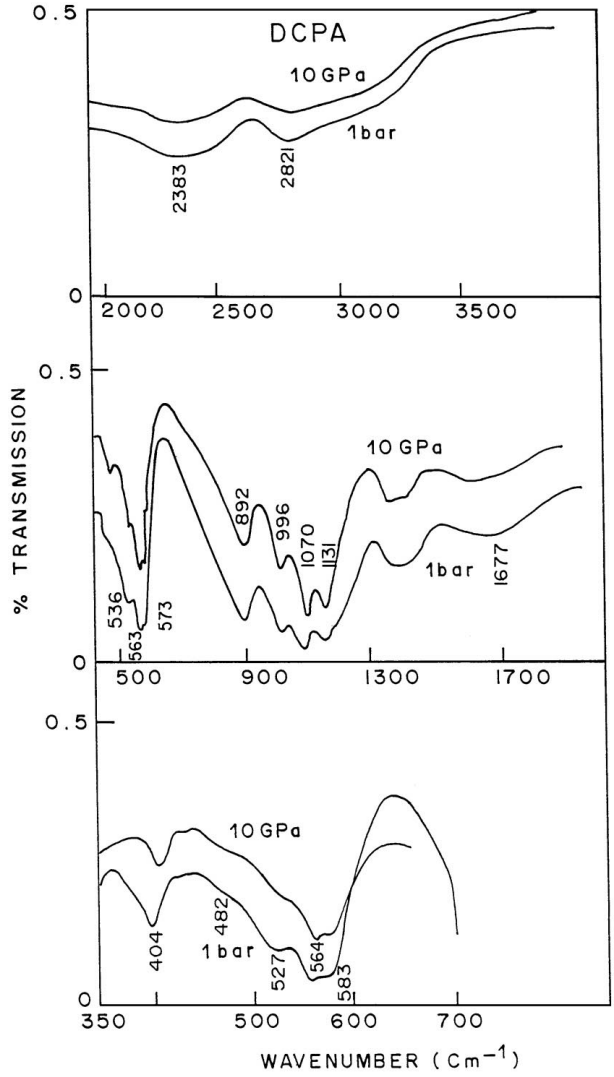

Figure 16 Effect of pressure on the FTIR spectrum of $CaHPO_4$.

5. Conclusions

In the loosely packed structures of these calcium phosphates, the PO_4 groups neither share the corners nor the edges but are held together by the cations and water molecules present. At high pressures, the structures of HTCP, HA and α TCP, which are made up of columns of Ca-O and PO_4 groups, collapse begins along the column axis. Among these materials HA and α TCP amorphizes at about 10 GPa, while HTCP has the lowest pressure of amorphization $\sim$2 GPa. It can be noted that although the structure of α TCP has Ca atom vacancies, its pressure of amorphization (P_2) is comparable to that of HA. In the structure of HTCP, the Ca atom vacancies and water molecules which are statistically distributed over the allowed sites in the HA type structure, on the other hand shows low P_2 viz., 2 GPa. High pressure studies on potash alum has shown that P_2 is reduced substantially when the concentration of defects is high. This does not however seem to happen in case of α TCP. All the three materials show similar infrared spectra associated with the PO_4 group. The wide PO_4 band exhibits pronounced narrowing on transition to amorphous state. In case of HA and HTCP in crystalline phase the water is hydrogen bonded and the internal stretching mode of OH is present at 3561 cm^{-1} and 3565 cm^{-1} respectively in the crystalline phase. In amorphous phase we

observe two sharp bands at 3561 and 3673 cm^{-1} in HA and 3565 and 3678 cm^{-1} in HTCP due to the presence of bonded as well as free water in this phase.

The crystal structures of DCPD and DCPA contain sheets of composition -Ca-PO_4-Ca-PO_4-. At high pressures these structures collapse in the plane of the sheet as the transition from c→a takes place. The pressure amorphized phase remains highly anisotropic at intermediate pressures. The pressure of c→a transition is lower in DCPA compared to DCPD. Both DCPD and DCPA have low symmetry and they show similar PO_4 absorption bands. DCPA which has the lowest symmetry does not show significant changes in the infrared spectra on amorphization. In DCPD, there are additional bands due to two distinct types of water molecules. The OH stretching modes do not change at the c→a transition, but the OPO bend modes below 550 cm^{-1} show many changes. We found that below 550 cm^{-1} the infrared spectra of DCPD in amorphous phase resembles that of HA in the crystalline phase and conversely the spectra of DCPD in the crystalline phase resembles that of HA in the amorphous phase.

Acknowledgements

We are very grateful to Dr. P. V. Ravindran of Analytical Chemistry Division for the DTA-TG experiments.

References

1. Bioceramics: Material Characteristics Verses in vivo Behaviour, Vol. 523, edited by P. Decheyne and L. E. Lemons (Ann. N.Y. Acad. Sci., 1988).
2. M. WANG, D. PORTER and W. BONFIELD, *Br. Ceram. Trans.* **93** (1994) 91.
3. T. S. CHIM, D. C. WU, M. P. HUNG and C. P. WANG, *J. Mater. Res.* **11** (1996) 962.
4. T. NAKAMURA, T. YAMAMURO, S. HIGASHI, T. KOKUDO and S. ITOO, *J. Biomed. Res.* **19** (1985) 685.
5. K. KURASHINA, H. KURITA, M. HIRANO, J. M. A. DE BLIEK, C. P. A. T. KLIEN and K. DE GROOT, *J. Mater. Sci. Mater. Med.* **6** (1995) 340.
6. F. C. M. DRIESSENS, M. G. BOLTONG, O. BERMUDEZ, J. A. PLANELL, M. P. GINEBRA and E. FERNANDEZ, *ibid.* **5** (1994) 164.
7. M. P. GINEBRA, M. G. BOLTONG, E. FERNANDEZ, J. A. PLANNEL and F. C. M. DRIESSENS, *ibid.* **6** (1995) 612.
8. D. M. ROY and S. K. LINECHANN, *Nature* **247** (1974) 252.
9. S. N. VAIDYA, C. KARUNAKARAN, B. M. PANDE, N. M. GUPTA, R. K. IYER and S. B. KARWEER, *J. Mater. Sci.* **32** (1997) 3213.
10. S. N. VAIDYA, V. SUGANDHI and A. P. ROY, Int. Conf. on Condensed Matter Physics Under High Pressure, Mumbai, 1996, published in "Advances in High Pressure Research in Condensed Matter," ed. by S. K. Sikka, Satish C. Gupta and B. K. Godwal (National Institute Science Communication, New Delhi 1997) pp. 139–145.
11. S. K. EKBUNDIT, K. LEINENWEBER, J. L. YARGER, J. S. ROBINSON, M. VERHELST-VOORHEES and G. H. WOLF, *J. Sol. Stat. Chem.* **126** (1996) 300.
12. M. B. KRUGER and R. JEANLOZ, *Science* **249** (1990) 647.
13. C. MEADE and R. JEANLOZ, *Geophysical Research Letter* **17** (1990) 1157.
14. S. K. SIKKA and S. M. SHARMA, *Curr. Sci.* **63** (1992) 317.
15. S. M. SHARMA and S. K. SIKKA, *Progress in Mater. Sci.* **40** (1996) 1.
16. C. A. BADDIEL and E. E. BERRY, *Spectrochim. Acta* **22** (1966) 1407.
17. A. BERTOLUZZA, M. A. BATTAGLIA, R. SIMONI and D. A. LONG, *J. Raman, Spectrosc.* **14** (1983) 178.
18. F. CASCIANI and R. D. CONDRATE, *Sr., Spectro. Letters* **12** (1979) 699.
19. V. VIJAYAKUMAR, S. N. VAIDYA, E. V. SAMPATHKUMARAN and L. C. GUPTA, *High Temp.-High Press.* **12** (1980) 649.
20. S. N. VAIDYA, D. K. JOSHI and C. KARUNAKARAN, *Ind. J. Technol.* **14** (1976) 679.
21. F. H. LIN, T. L. HARN and M. H. HON, *Ceram. Int.* **15** (1989) 351.
22. A. S. POSNER, A. PERLOFF and A. F. DIORO, *Acta Cryst.* **11** (1958) 308.
23. LANDOLT-BORNSTEIN, "Crystal Structure Data of Inorganic Compounds," Vol. 7c 2, (Springer, Berlin, 1979) pp. 202, 248.
24. K. SUDARSHAN and R. A. YOUNG, *Acta Cryst.* **B25** (1969) 1534.
25. M. I. KAY, R. A. YOUNG and A. S. POSNER, *Nature* **204** (1964) 1050.
26. T. SAKUNTALA and A. K. ARORA, communicated.
27. M. MATHEW, L. W. SCHROEDER, B. DICKENS and W. E. BROWN, *Acta Cryst.* **B33** (1977) 1325.
28. C. A. BEEVERS, *Acta Cryst.* **11** (1958) 273.
29. G. MACLENNAN and C. A. BEEVERS, *ibid.* **8** (1955) 579.

Received 24 October 1997
and accepted 8 February 1999